Available online at www.sciencedirect.com
ScienceDirect
Solar Energy 85 (2011) 12–18
SOLAR ENERGY
www.elsevier.com/locate/solener

Parameter extraction from *I–V* characteristics of PV devices

Erees Queen B. Macabebe [a,b,*], Charles J. Sheppard [c], E. Ernest van Dyk [b]

[a] *Department of Electronics, Computer and Communications Engineering, Ateneo de Manila University, Loyola Heights, Quezon City 1108, Philippines*
[b] *Department of Physics and Centre for Energy Research, Nelson Mandela Metropolitan University, PO Box 77000, Port Elizabeth 6031, South Africa*
[c] *Department of Physics, University of Johannesburg, PO Box 524, Auckland Park 2006, South Africa*

Received 25 May 2010; received in revised form 29 October 2010; accepted 8 November 2010
Available online 7 December 2010

Communicated by: Associate Editor Takhir Razykov

Abstract

Device parameters such as series and shunt resistances, saturation current and diode ideality factor influence the behaviour of the current–voltage (*I–V*) characteristics of solar cells and photovoltaic modules. It is necessary to determine these parameters since performance parameters are derived from the *I–V* curve and information provided by the device parameters are useful in analyzing performance losses. This contribution presents device parameters of $CuIn(Se,S)_2$- and $Cu(In,Ga)(Se,S)_2$-based solar cells, as well as, $CuInSe_2$, mono- and multicrystalline silicon modules determined using a parameter extraction routine that employs Particle Swarm Optimization. The device parameters of the $CuIn(Se,S)_2$- and $Cu(In,Ga)(Se,S)_2$-based solar cells show that the contribution of recombination mechanisms exhibited by high saturation current when coupled with the effects of parasitic resistances result in lower maximum power and conversion efficiency. Device parameters of photovoltaic modules extracted from *I–V* characteristics obtained at higher temperature show increased saturation current. The extracted values also reflect the adverse effect of temperature on parasitic resistances. The parameters extracted from *I–V* curves offer an understanding of the different mechanisms involved in the operation of the devices. The parameter extraction routine utilized in this study is a useful tool in determining the device parameters which reveal the mechanisms affecting device performance.

Keywords: Parameter extraction; Particle swarm optimization; Solar cells; PV modules; Device parameters; Module performance

1. Introduction

The open-circuit voltage (V_{oc}), short circuit current (I_{sc}), maximum power (P_{max}), fill factor (*FF*) and conversion efficiency (η_c) are performance parameters derived from the light current–voltage (*I–V*) characteristic of the photovoltaic device. The effects of series (R_s) and shunt (R_{sh}) resistances, saturation current (I_o) and ideality factor (n) on the behaviour of the *I–V* characteristics need to be investigated to understand their effect on the performance of the devices.

In this contribution, a parameter extraction routine based on Particle Swarm Optimization (PSO) was developed to rapidly extract the device parameters R_s, R_{sh}, I_o and n from the *I–V* characteristic of several photovoltaic devices. Several methods to determine these parameters have been proposed, extensively discussed and compared in other publications (Jervase et al., 2001; Chegaar et al., 2006; Bouzidi et al., 2007). Results obtained using a PSO routine which were rapidly extracted, within a few seconds, from the *I–V* curve of different devices are presented in this paper. PSO as an algorithm for solar cell extraction has been published recently and compared to genetic algorithm by another set of authors (Meiying et al., 2009). The difference of the method utilized in this contribution is that the

* Corresponding author at: Department of Electronics, Computer and Communications Engineering, Ateneo de Manila University, Loyola Heights, Quezon City 1108, Philippines.
E-mail addresses: emacabebe@ateneo.edu (Erees Queen B. Macabebe), cjsheppard@uj.ac.za (C.J. Sheppard), ernest.vandyk@nmmu.ac.za (E.E. van Dyk).

0038-092X/$ - see front matter © 2010 Elsevier Ltd. All rights reserved.
doi:10.1016/j.solener.2010.11.005

PSO routine explores a larger solution space as the boundary conditions imposed are not as rigid as in the method published by Meiying et al. Also, the extractions require less number of iterations, despite the large search space, which makes the routine more efficient.

The well-known one- and two-diode solar cell models were considered to determine the device parameters using the PSO routine. However, it was found in an earlier work (Macabebe and van Dyk, 2008) that the two-diode model provides a better representation of the solar cell's *I–V* characteristics. Hence, the two-diode model was preferred and the parameters of the model were determined to correlate the device and performance parameters of $CuIn(Se,S)_2$- and $Cu(In,Ga)(Se,S)_2$-based solar cells, and $CuInSe_2$, monocrystalline silicon (Mono-Si) and multicrystalline silicon (Multi-Si) photovoltaic modules.

2. Parameter extraction

To account for recombination processes influencing the behaviour of the *I–V* characteristics, the two-diode model was considered. Fig. 1 shows two-diode model equivalent circuit when the solar cell is under light conditions. The diodes D_1 and D_2 represent the two processes governing the solar cell. These could be diffusion and/or any of the recombination processes involved in solar cell operations. The voltage V_D across the junction of the device is equal to $V + IR_s$ where V and I are the device's measured output voltage and current, respectively, and IR_s represents series resistance losses. The *I–V* characteristic is described by the equation

$$I = I_L - I_{o1}\left[\exp\frac{q}{n_1 kT}(V + IR_s) - 1\right] - I_{o2}\left[\exp\frac{q}{n_2 kT}(V + IR_s) - 1\right] - \frac{V + IR_s}{R_{sh}}. \quad (1)$$

where I_L is the photo-generated current, I_{o1} and I_{o2} are the saturation currents dependent on the recombination process indicated by the diode ideality factors n_1 and n_2.

Parameters of the model were determined by approximation and iteration using a PSO-based extraction routine (Macabebe, 2009). PSO is an evolutionary technique motivated by the simulation of social behaviour observed in flocks of birds and schools of fish (Eberhart and Kennedy, 1995). In PSO each particle is randomly initialized as a possible solution. A particle is described as a position with coordinates equal to the values of the parameters. The position of each particle has a velocity. This velocity directs the particle's motion through the solution space which refers to the combination of parameter values. The velocity varies in each iteration and is calculated using the equation

$$v_k = w * v_{k-1} + c_1 * rand() * (pbest_{k-1} - p_{k-1}) + c_2 * rand() * (gbest - p_{k-1}). \quad (2)$$

The subscript k in Eq. (2) represents the kth iteration and w is the inertia weight. The introduction of inertia weight w allowed global exploration preventing the optimizer from being trapped at a local minimum (Shi and Eberhart, 1998). The variable v_k is the particle's current velocity and v_{k-1} is its previous velocity, p_k and p_{k-1} are the current and previous position (solution), respectively, $pbest_{k-1}$ and $gbest$ are defined as personal best and global best, respectively. *Rand( )* is a randomly generated number between 0 and 1, c_1 and c_2 are learning factors equal to two and they control the maximum step size. The velocity is clamped to a range $[-v_{max}, v_{max}]$ to control the particle movement within the search space. The position is then updated using the equation $p_k = p_{k-1} + v_k$.

Each particle searches the solution space for the combination that optimizes the fitness function. The resulting fitness value is the attribute of the particle's current position. For the solar cell parameter extraction routine, the fitness function to be minimized is the mean residual error defined by Eq. (3) where I is the measured current and Ic is the computed current given by the right-side of Eq. (1).

$$\overline{res} = \frac{\sum_{i=1}^{N}\sqrt{(I_i - Ic_i)^2}}{N} \quad (3)$$

To make the routine efficient, Eq. (2) utilized a dynamic inertia weight function w' instead of w. The function $w' = wu^{-k}$ proposed by Jiao et al. has the following conditions: (a) w takes a value between 0 and 1, (b) u is a value between 1.0001 and 1.005, and (c) k is the iteration number. This function decreases as the iterative generation increases (Jiao et al., 2008). The flow diagram of the method utilized to extract the parameters of the two-diode model is illustrated in Fig. 2.

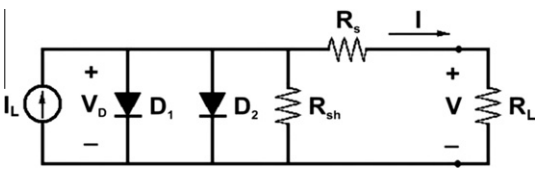

Fig. 1. Two-diode solar cell equivalent circuit model under light conditions.

3. Experimental details

Particle Swarm Optimization as an algorithm to extract solar cell parameters has been implemented using Matlab, compared and was found to be more accurate than Genetic Algorithm (Meiying et al., 2009). The PSO parameter extraction routine that is presented here was also implemented in Matlab but using an ordinary desktop computer with 3.40 GHz CPU and 2 GB of RAM. To test accuracy of the extraction method, typical solar cell parameters were simulated using the two-diode model. However, residual error between 0.00001 and 0.01was introduced to the simulated *I–V* curves to test how the algorithm handles possible measurement errors in actual data. Several sets of parameters were extracted using the synthetic *I–V* curve and the extracted values were compared to the parameter

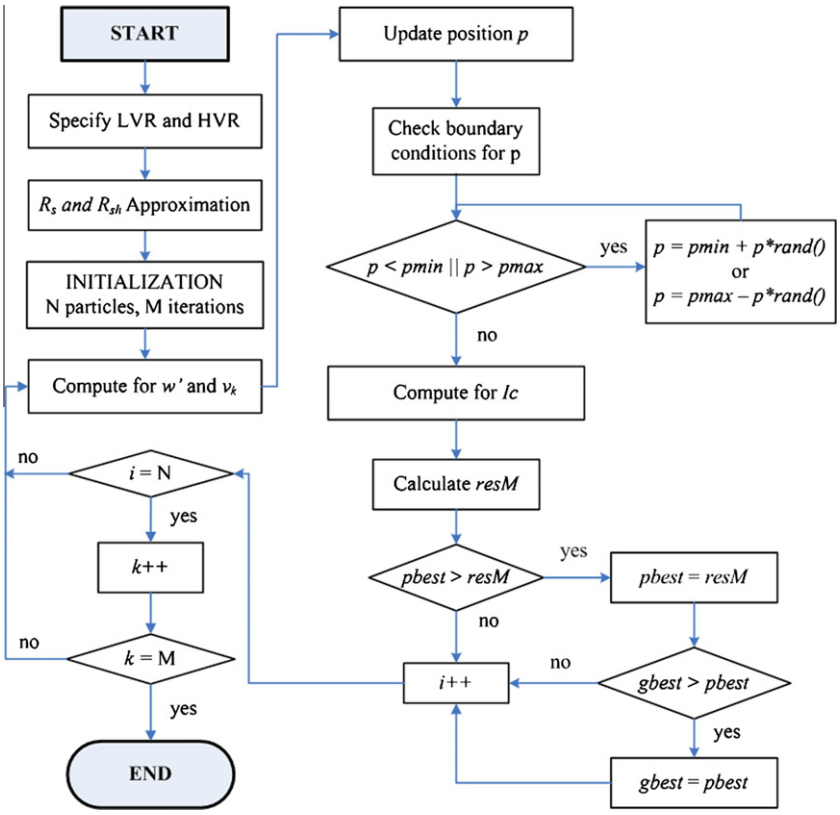

Fig. 2. Flowchart of the modified PSO parameter extraction method utilizing the illuminated *I–V* characteristic of solar cells.

values used in the simulation. Also, in this test for accuracy, the population size was varied from 50 to 100 particles and for each size the number of iterations was varied from 20 to 100, much less than that of the earlier work (Meiying et al., 2009). The boundary conditions for the parameters are as follows: $1 < n < 5$ and $0 < I_o < 1$. The range for R_s and R_{sh} was set at $\pm 70\%$ of the value determined by approximation using the slopes at I_{sc} and the slope at V_{oc}, respectively.

Applying the PSO method to estimate the device parameters of actual photovoltaic devices of different types and under different conditions, the *I–V* characteristics of solar cells and PV modules were considered. The $CuIn(Se,S)_2$- and $Cu(In,Ga)(Se,S)_2$-based solar cells were manufactured using the two-step process (Sheppard and Alberts, 2006). The current density–voltage (*J–V*) characteristics of the solar cells were measured in the dark and under standard measurement conditions: irradiance of 1000 W/m^2, A.M. 1.5 solar spectrum, and device temperature of 25 °C. The $CuInSe_2$, Mono-Si and Multi-Si modules are commercially available. Thirty-three (33) monolithically integrated solar cells comprised the 5 W-$CuInSe_2$ modules. The 50-W crystalline silicon modules are composed of thirty-six (36) series-connected solar cells. The *I–V* characteristics of the modules were obtained under outdoor conditions and using a flash solar simulator. All outdoor measurements were taken on a clear day between 11:00 and 13:00 H. Measurements were corrected to 1000 W/m^2. Module temperature during outdoor measurements varied between 33.4 and 53.7 °C while indoor measurements using the solar simulator registered module temperature variation between 20.1 and 22.5 °C. The flashlight solar simulator utilized a Xenon flashlamp spectrally filtered to AM 1.5. During *I–V* measurement, the intensities were set between 1200 and 1450 W/m^2 and the *I–V* curves were later corrected to 1000 W/m^2. This was done to avoid lost points near V_{oc} which occurs during curve transfer towards higher intensities (Optosolar). The *I–V* curves were not corrected for temperature but module temperature during measurement was obtained and noted in the results.

4. Results and discussion

To verify the accuracy of the PSO routine, parameters from a synthetic *I–V* data was extracted. Plots of the distribution of the extracted R_s, R_{sh}, I_{o1} and n_1 values are shown in Fig. 3. It is obvious that when the mean residual error is reduced, the accuracy of the value determined by the extraction routine is higher as seen by the decreasing deviation when the mean residual error is decreased. The accuracy of the extracted values and errors of I_{o1} and n_1 are dependent on the accuracy of R_s as seen in Fig. 3 where figures (a), (c) and (d) follow the same trend. On the other hand, the parameters I_{o2} and n_2 acquired the largest errors and the distributions of values for these two parameters follow the trend exhibited by R_{sh}. These large errors are partly attributed to the errors introduced when the synthetic *I–V* data was generated. Note that usually the

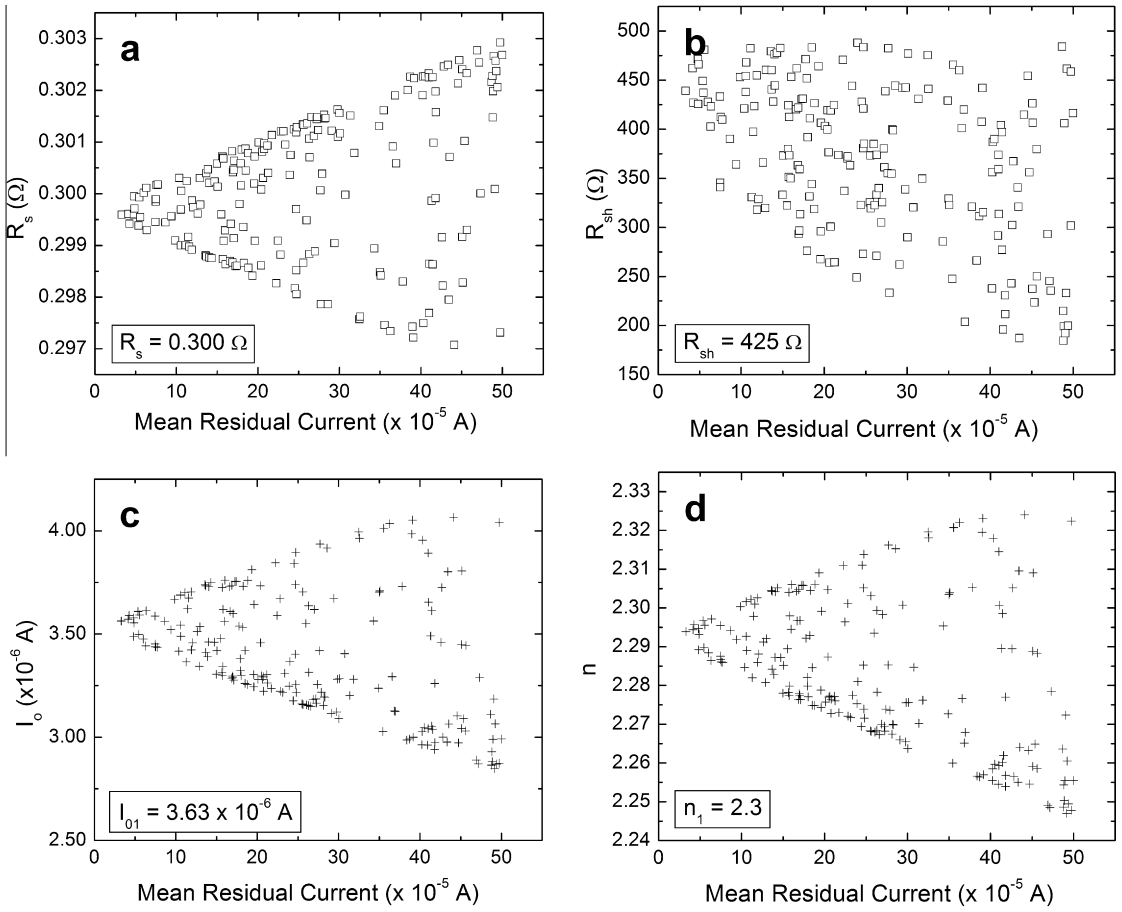

Fig. 3. Distribution of the extracted values for: (a) R_s, (b) R_{sh}, (c) I_{o1} and (d) n_1 as a function of the mean residual error.

contribution of the second exponential term to the dark current is very small and this residual current is also affected by the R_{sh} term in Eq. (1) which represents leakage current. Hence, the accuracy of I_{o2} and n_2 is greatly dependent on the accuracy of the extracted R_{sh} value. This accuracy can be improved by reducing the boundary condition or range of R_{sh} during parameter extraction.

The light current density–voltage (J–V) characteristics of the laboratory manufactured CuIn(Se,S)$_2$- and Cu(In,-Ga)(Se,S)$_2$-based solar cells are shown in Fig. 4. The device and performance parameters are listed in Tables 1 and 2, respectively. The parameter J_L is the photo-generated current density while J_{o1} and J_{o2} are the saturated current densities.

Comparing the two devices, the Cu(In,Ga)(Se,S)$_2$-based solar cell generated more carriers resulting in higher J_L and J_{sc}. The effects of parasitic resistances are greater in the CuIn(Se,S)$_2$-based solar cell indicated by higher R_s and lower R_{sh}. Moreover, the diode ideality factors and J_{o2} of the device are much higher than that of Cu(In,Ga)(Se,S)$_2$-based solar cell. As a consequence, the contribution of recombination mechanisms exhibited by higher saturation current, when coupled with the effects of parasitic resistances, result in lower maximum power and conversion efficiency.

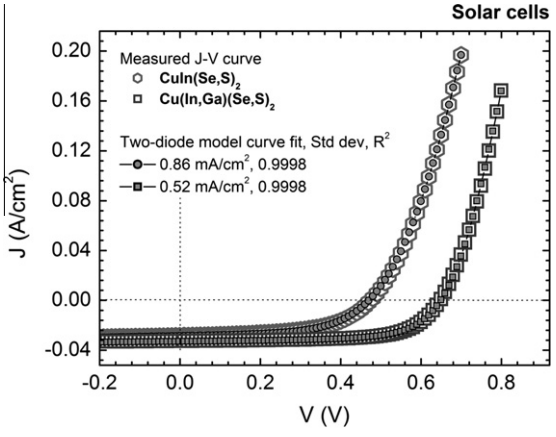

Fig. 4. Light J–V curves of CuIn(Se,S)$_2$ and Cu(In,Ga)(Se,S)$_2$-based solar cells with two-diode model fitted curves using the PSO method.

The light I–V characteristics of the CuIn(Se,S)$_2$, Mono-Si and Multi-Si modules were obtained indoor using a solar simulator and outdoor using a standardized measurement system. The light I–V curves of the modules are shown in Fig. 5 with the two-diode model fitted curves. The I–V curves of the CuInSe$_2$ and the 50-W Multi-Si module in Fig. 5 shows that I_{sc} is slightly higher when the modules were outdoor. The detrimental effect of increased module

Table 1
Device parameters extracted from the J–V characteristics of CISS and CIGSS solar cells using the PSO method.

Device	J_L (mA/cm^2)	R_s (Ω-cm^2)	R_{sh} (Ω-cm^2)	J_{o1} (A/cm^2) × 10^{-6}	n_1	J_{o2} (A/cm^2) × 10^{-7}	n_2
$CuIn(Se,S)_2$	28.66	0.415	172.09	24.12	4.88	237.45	2.64
$Cu(In,Ga)(Se,S)_2$	32.99	0.382	359.95	24.25	4.26	0.036	1.62

Table 2
Performance parameters of CISS and CIGSS solar cells.

Device	J_{sc} (mA/cm^2)	V_{oc} (mV)	J_{mpp} (mA/cm^2)	V_{mpp} (mV)	FF	η_c (%)
$CuIn(Se,S)_2$	28.51	474.77	21.71	342.56	0.55	7.44
$Cu(In,Ga)(Se,S)_2$	32.61	647.42	27.77	514.44	0.68	14.29

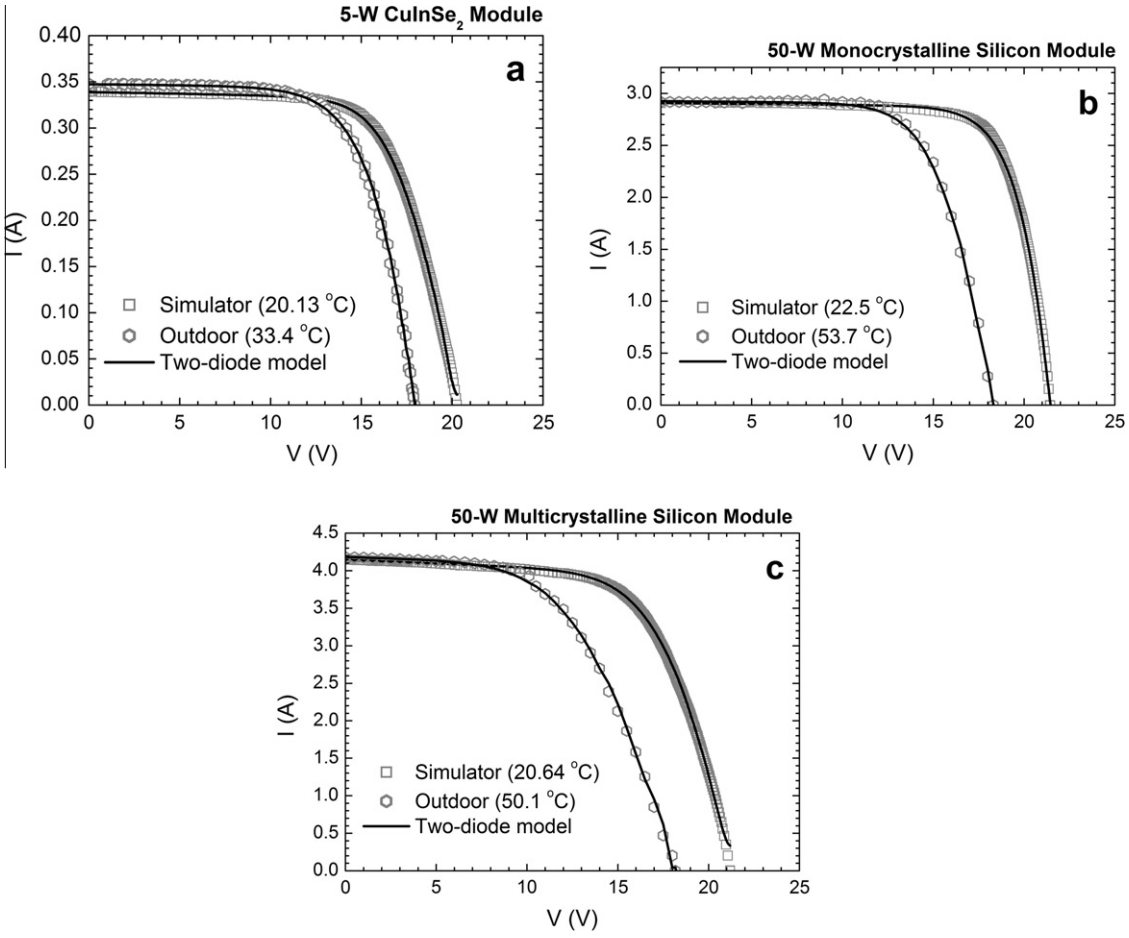

Fig. 5. Light I–V curves obtained outdoor and indoor using the solar simulator with the two-diode model fitted curves for: (a) the 5-W $CuInSe_2$, (b) the 50-W Mono-Si and (c) the 50-W Multi-Si modules.

temperature, however, becomes obvious at the knee causing the V_{oc} to drastically decrease. This behaviour is due to increased dark and recombination currents with increasing temperature. The effect of increased R_s is apparent on the 50-W Mono-Si and the 50-W Multi-Si in Fig. 5b and c judging from the slope of the outdoor I–V plots near V_{oc}. The temperature difference between the indoor and outdoor measurements for the two 50-W modules are the greatest, hence, R_s is greater due to increased resistance of the metallic contacts with increasing temperature.

The device parameters extracted using the PSO routine are listed in Table 3 and the performance parameters are found in Table 4. For the $CuInSe_2$ module, exposure to solar radiation for a few minutes prior to measurements improved absorption and slightly increased I_L and I_{sc}. Despite the slight increase in I_{o1}, parameters such as R_s and R_{sh} improved. This resulted in improved fill factor but the effect of temperature on V_{oc} decreased P_{max} which caused the 10% drop on the conversion efficiency to 8.43% from 9.39% at room temperature.

Table 3
Device parameters of the PV modules extracted using the PSO routine from illuminated *I–V* curve obtained indoor and outdoor. Values are average per cell.

Devices	I_L (A)	R_s (mΩ)	R_{sh} (Ω)	I_{o1} (A)	n_1	I_{o2} (A)	n_2
Indoor							
5-W $CuInSe_2$	0.34	186.03	85.03	8.10×10^{-6}	4.40	1.82×10^{-8}	1.46
50-W Mono-Si	2.91	4.22	17.66	2.10×10^{-7}	1.42	5.66×10^{-10}	1.81
50-W Multi-Si	4.17	15.33	2.91	5.58×10^{-6}	1.74	1.76×10^{-9}	7.42
Outdoor							
5-W $CuInSe_2$	0.35	73.48	141.28	4.67×10^{-10}	2.02	3.24×10^{-6}	1.78
50-W Mono-Si	2.93	15.58	18.68	2.12×10^{-6}	1.28	3.23×10^{-8}	3.04
50-W Multi-Si	4.21	23.86	4.04	1.21×10^{-4}	1.74	5.33×10^{-10}	4.78

Table 4
Performance parameters of the PV modules obtained from the indoor and outdoor *I–V* curve.

Devices	I_{sc} (A)	V_{oc} (V)	I_{max} (A)	V_{max} (V)	P_{max} (W)	FF	η_c (%)	Temp (°C)
Indoor								
5-W $CuInSe_2$	0.34	20.25	0.31	15.48	4.73	0.69	9.39	20.1
50-W Mono-Si	2.91	21.43	2.68	17.81	47.68	0.77	10.99	22.5
50-W Multi-Si	4.15	21.19	3.61	15.73	56.76	0.65	9.56	20.6
Outdoor								
5-W $CuInSe_2$	0.35	18.09	0.30	14.17	4.25	0.67	8.43	33.4
50-W Mono-Si	2.91	18.32	2.49	14.50	36.06	0.68	8.31	53.7
50-W Multi-Si	4.18	19.45	3.32	13.24	43.95	0.54	7.40	50.1

In Table 3, the ideality factors of the crystalline silicon modules obtained from indoor *I–V* curve show that recombination through defects and traps in the depletion region is the dominant process. This is usually the case for crystalline solar cells operating at room temperature (Nelson, 2003). The average ideality factor of each solar cell in the modules falls between 1 and 2, except for the 50-W Multi-Si module where the second exponential term indicates bulk recombination or recombination enhanced by field-assisted tunneling resulting in $n > 2$. However, the contribution of I_{o2} and n_2 to the dark current in the 50-W Multi-Si module is a few orders of magnitude lower than I_{o1} and n_1. Thus, recombination in the depletion region is also the dominant recombination process in the 50-W Multi-Si module.

The device parameters extracted from the *I–V* curve obtained outdoor show that, in general, recombination in the depletion region remained dominant. However, the saturation currents increased since they are derived from temperature-dependent quantities such as the diffusion coefficient D, carrier lifetime τ and the intrinsic carrier concentration n_i (Sze, 1981). This resulted in increased recombination currents which reduced V_{oc}, P_{max} and FF (see Table 4). Also, the extracted values reflect the adverse effect of temperature on parasitic resistances.

5. Conclusion

The parameter extraction routine based on Particle Swarm Optimization presented in this paper can rapidly extract and provide a good estimate of the device parameters obtained from the *I–V* curves of solar cells and PV modules. The parameters extracted from the *I–V* curves offer an understanding of the different mechanisms involved in the operation of the devices. For the solar cell samples, the high saturation current due to increased recombination in the $CuIn(Se,S)_2$ solar cell, coupled with reduced shunt resistance resulted in a lower V_{oc}, a lower FF and, consequently, lower conversion efficiency. For the modules, indoor *I–V* measurements show that recombination in the depletion region dominate Si devices at room temperature. Under outdoor conditions, module temperature increased which caused the general increase in the saturation currents of the PV modules. The detrimental effects of parasitic resistances on the 50-W Si modules increased as well, reducing the overall performance of the devices. Outdoor exposure slightly improved the *I–V* curve of the $CuInSe_2$ module near I_{sc}. However, increased recombination reduced V_{max} which resulted in lower P_{max}, FF and η_c. The parameter extraction routine utilized in this study is a useful tool in determining the device parameters which reveal the mechanisms affecting device performance.

Acknowledgements

The authors would like to acknowledge the Nelson Mandela Metropolitan University and the Schlumberger Foundation Faculty for the Future Program for supporting E.Q.B. Macabebe.

References

Bouzidi, K., Chegaar, M., Bouhemadou, A., 2007. Solar cells parameters evaluation considering the series and shunt resistance. Solar Energy Materials and Solar Cells 91, 1647–1651.

Chegaar, M., Azzouzi, G., Mialhe, P., 2006. Simple parameter extraction method for illuminated solar cells. Solid-State Electronics 50, 1234–1237.

Eberhart, R.C., Kennedy, J. (1995). A new optimizer using particles swarm theory, In: Proc. of the Sixth International Symposium on Micro Machine and Human Science, 4–6 Oct, Nagoya, Japan, pp. 39–43.

Jervase, J.A., Bourdoucen, H., Al-Lawati, A., 2001. Solar cell parameter extraction using genetic algorithms. Measurement Science and Technology 12, 1922–1925.

Jiao, B., Lian, Z., Gu, X., 2008. A dynamic inertia weight particle swarm optimization algorithm. Chaos, Solitons Fractals 37, 698–705.

Macabebe, E.Q.B. (2009). Investigation of device and performance parameters of photovoltaic devices. PhD Thesis, Nelson Mandela Metropolitan University, Port Elizabeth, ZA.

Macabebe, E.Q.B., van Dyk, E.E., 2008. Parameter extraction from dark current–voltage characteristics of solar cells. South African Journal of Science 104, 401–404.

Meiying, Y., Xiaodong, W., Yousheng, X., 2009. Parameter extraction of solar cells using particle swarm optimization. Journal of Applied Physics 105, 094502.

Nelson, J., 2003. The Physics of Solar cells. Imperial College Press, London.

Optosolar GmbH Module tester for large area PV modules for building integration. Product Manual, Merdingen, Germany.

Sheppard, C.J., Alberts, V., 2006. Deposition of single-phase CuIn(Se, S)2 thin films from the sulfurization of selenized CuIn alloys. Journal of Physics D: Applied Physics 39, 3760–3763.

Shi, Y., Eberhart, R.C. (1998). Parameter selection in particle swarm optimization. In: Proceedings of the Seventh Annual Conference on Evolutionary Programming, March 24–27, California, USA <http://www.engr.iupui.edu/~shi/PSO/Paper/EP98/psof6/ep98_pso.html> (accessed 28.07.09).

Sze, S.M., 1981. Physics of Semiconductor Devices, second ed. Wiley, New York.